# Electromagnetic Bandgap Design for Power Distribution Network Noise Isolation in the Glass Interposer

Youngwoo Kim, Jinwook Song, Subin Kim and Joungho Kim
Department of Electrical Engineering
KAIST
Daejeon, South Korea
youngwoo@kaist.ac.kr

Venky Sundaram and Rao Tummala
3D System Packaging Research Center
Gerogia Institute of Technology
Atlanta, GA 30332, USA
vs24@mail.gatech.edu

Jonghyun Cho
EMC Lab
MST
Rola, MO USA
chojon@mst.edu

*Abstract*—**2.5-Dimensional integration based on glass interposer technology is a potential means of achieving high-bandwidth and high-integration density electrical systems. Ultra-low loss glass substrate enables high-frequency signaling but this low loss substrate is vulnerable to the noise suppression in the power distribution network (PDN). Electromagnetic Band-gap (EBG) structures in the PDN are well-known techniques to suppress the PDN noise. We first designed and fabricated EBG structures in the glass interposer PDN and analyzed effectiveness of these EBG structures for the noise suppression in the PDN.**

***Keywords- Electromagnetic Bandgap, Glass Interposer, Power Distribution Network, Power Noise***

## I. INTRODUCTION

2.5-Dimensional integration based on Glass interposer is a potential means of achieving high-bandwidth and high-integration density electrical systems. Glass interposers have several advantages such as excellent dimensional stability, closely-matched coefficient of thermal expansion (CTE) to silicon dies to be mounted, availability of glass substrates in large and thin panel sizes compared to that of silicon wafers and more importantly, excellent electrical resistivity of glass substrate which will contribute to low signal loss up to GHz range [1-2]. Therefore 2.5-D integration based on Glass interposer is a potential means of achieving high-bandwidth and high-integration density electrical systems at the same time lowering the manufacturing cost.

However, although low-conductivity of the glass interposer substrate provides low channel loss up to high frequency ranges, this low substrate conductivity is vulnerable to the noise suppression in power distribution network (PDN) of the glass interposer. PDN is a path where power current flows from a voltage regulator to the ICs. When these ICs operate at the same time, they generate simultaneous switching noise (SSN) in the PDN and this noise many propagate along the PDN causing many signal/power integrity and EMI radiation issues [3]. Due to the low substrate loss, this noise in the PDN may propagate further and may deteriorate performance of the ICs in the PDN. Also low loss glass substrate generates sharp PDN impedance peaks at the PDN resonance frequencies. At these frequencies, more noise is induced from the signal through glass via (TGV) to the PDN [4]. Fig. 1 shows the noise propagation issues in the glass interposer PDN.

Electromagnetic band-gap structures are well known techniques to suppress noise propagation in the PDN. We for the first time designed and fabricated glass interposer PDN with EBG structures to suppress the noise in the PDN. We simulated and measured the frequency ranges where noise could be isolated depending on the structures and dimensions of the designed EBG structures. In case of the mushroom type EBG in the glass interposer PDN, increasing the number of the patches widen the band-gap region. When the number of patches is fixed we have found that compared to altering the number of patches, size variation effect seems minimal. In cased of the EBG with defected structure, we changed the number of defects and the band-gap increased until certain point.

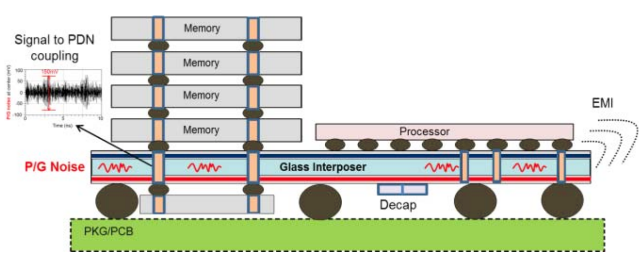


Fig. 1. Noise propagation in the glass interposer PDN is depicted

978-1-5090-1204-6/16 $31.00 © 2016 IEEE
DOI 10.1109/ECTC.2016.169

## II. DESIGN RULES AND DESCRIPTION OF THE DESIGNED ELECTROMAGNETIC BANDGAP IN THE GLASS INTERPOSER POWER DISTRIBUTION NETWORK

We designed and fabricated glass interposer PDNs with various types of EBG structures. EBG can be designed by repeating the same structures in the PDN. Since conventional PDN can be modeled into repeating unit cells [5-6], PDN with EBG can also be modeled with repeating unit cells. Each unit cell can be modeled into the capacitance, inductance and resistance of the PDN. By repeating these RLC networks, filter that can suppress noise propagation in the PDN can be achieved. Based on the designed EBG structures, we simulated, measured and analyzed the noise band-gap. The design was based on design rules of the glass interposer test vehicle fabrication processes.

### *A. Design Rules of the Glass Interposer*

Fig. 2 depicts the design rules of the glass interposer designed and fabricated. Total of four metal layers were processed for the interposer channels and PDN. Two metal layers were plated on each side of the EN-A1 glass substrate to form the double sided interposers. Since copper used for platting metal layers is not adhesive to the glass substrate, additional low loss polymer, ZS-100 is used between the glass substrate and the metal layers.

The physical dimensions and material properties of the glass interposer PDN with EBGs are summarized in Table I. The height of the glass substrate is ($h$) 100 μm and the thickness of the polymer layer 1 and 2 ($t_{pol\_1}$,$t_{pol\_2}$) are 22.5 μm and 17.5 μm respectively. Each metal layer consists of copper has thickness of 10μm. The TGV diameter ($d_{TGV}$) and TGV pad ($d_{pad\_TGV}$) are 60 μm and 90 μm respectively. Due to the limitation associated with the process and design rules, micro-via should be used and the diameter of the micro-via ($d_{\mu VIA}$) and TGV pad ($d_{pad\_\mu VIA}$) are 45 μm and 75 μm respectively. Relative permittivity of the glass substrate ($\varepsilon_{glass}$) and polymer ($\varepsilon_{pol}$) are 5.3 (at 2.4GHz) and 3 (at 10GHz) respectively with loss tangent ($tan\,\delta_{glass}$, $tan\,\delta_{pol}$) of 0.004(at 2.4GHz) and 0.005(at 10GHz).

### *B. Designed Glass Interposer PDN with EBGs*

In order to analyze the noise band-gap in the glass interposer PDN we designed various types of EBGs in the glass interposer PDN. Due to the fabrication failure for some test vehicles, it was impossible to measure and analyze all the designed and fabricated test vehicles. Also test vehicles in this glass interposer coupon include dummy pads and TGVs. To simulate all these components, it takes tremendous amount of time and computational resources, therefore simplified models were used for the simulation. Modeling of these EBGs and correlation between simulation, modeling and measurement remain for the future studies. In this work, we first simulate and analyze noise band-gap in the glass interposer PDN with various types of EBGs. We then measured the designed test vehicles and verify that proposed structures work as a noise suppression band-gap in the glass interposer PDN.

Fig. 3 shows glass interposer PDN with mushroom type EBG structures. The size of the PDN is 16mm by 16mm in x and y directions. Ground plane is designed on M1 and power plane is designed on M3 of the glass interposer. We altered the number of power patches, and the size (when altering the size, the number of power patches is fixed to four).

Fig. 4 shows glass interposer PDN with mushroom type EBGs and defected-power structures (DPS). The size of the PDN is 16mm by 16mm in x and y directions. Ground plane is designed on M1 and power plane is designed on M3 of

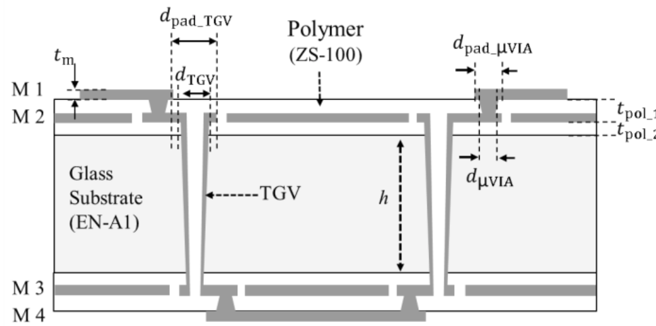


(a)

Fig. 2. Cross-sectional view of the glass interposer fabricated. Double sided glass interposer coupons consist of 4 metal layers, glass substrate, polymer, micro-vias and TGVs.

TABLE I
PHYSICAL DIMENSIONS AND MATERIAL PROPERTIES OF THE GLASS INTERPOSER

| | Symbol | Value |
|---|---|---|
| **Physical Dimensions** | $h$ | 100 μm |
| | $t_{pol\_1}$ | 22.5 μm |
| | $t_{pol\_2}$ | 17.5 μm |
| | $t_m$ | 10 μm |
| | $d_{TGV}$ | 60 μm |
| | $d_{pad\_TGV}$ | 90 μm |
| | $d_{\mu VIA}$ | 45 μm |
| | $d_{pad\_\mu VIA}$ | 75 μm |
| **Material Properties** | $\varepsilon_{glass}$ | 5.3 at 2.4GHz |
| | $\varepsilon_{pol}$ | 3 at 10GHz |
| | $tan\,\delta_{glass}$ | 0.004 at 2.4GHz |
| | $tan\,\delta_{pol}$ | 0.005 at 10GHz |
| | $\sigma_m$ | $5.8 \times 10^6$ σ/m |

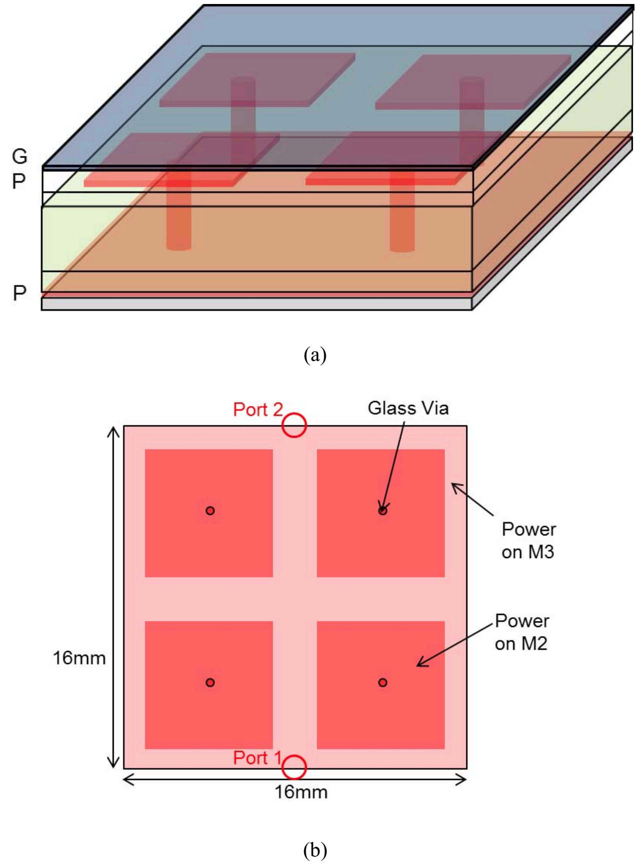


Fig. 3. (a) Glass interposer PDN with mushroom type EBG is depicted. (b) Power plane and power patches to from the EBG are shown. We changed the number and physical dimensions of the power patches

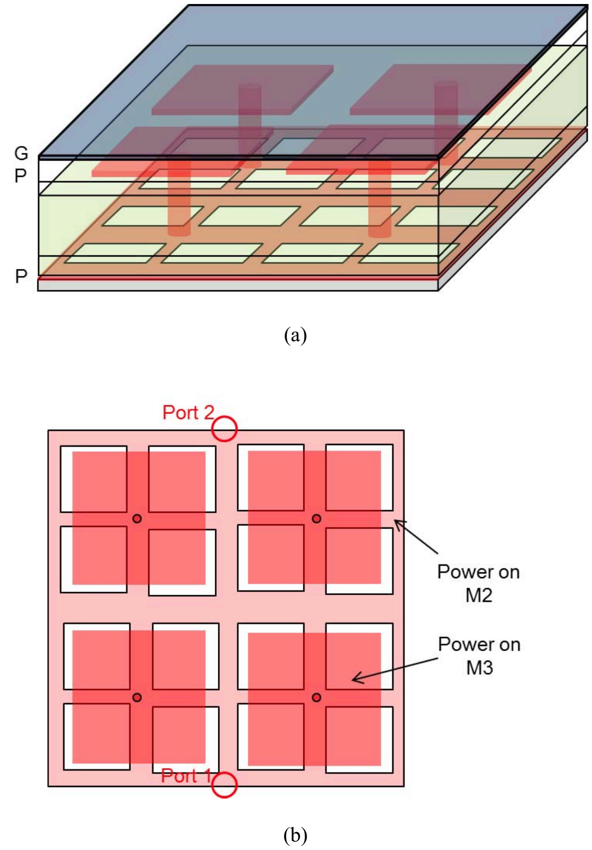


Fig. 4. (a) Glass interposer PDN with mushroom type EBG and defected-power structure is depicted. (b) We intentionally added defects in the power plane on M2.

the glass interposer. In this case, we fixed the number of power patches (7mm by 7mm) in M2 to four; however we added defects in the power plane designed in M3. To verify that proposed structures may work as an EBG, we fabricated glass interposer coupon with EBG patterns. Fig. 5 shows photo image of the fabricated glass interposer coupon with several test vehicles. We measured the test vehicles with VNA, model *N5230A* from Agilent Technologies, GS type microprobe and coaxial cables (W.L. Gore & Associates, Inc.)

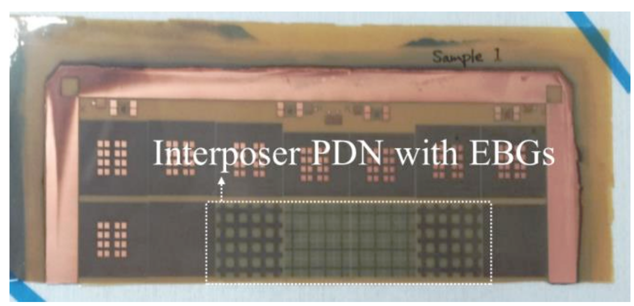


Fig. 5. Glass interposer coupon with EBG patterns are shown in white dotted line.

## III. Simulation Results and Analysis of Propsed EBG Design for the Glass Interposer

We first simulated and compared noise coupling coefficient of glass interposer PDN with and without mushroom type EBG. We defined the band-gap as a frequency range where the noise coupling coefficient is less then -40decibel in the PDN. Fig. 6 compares noise coupling coefficient with and without four power patches with 7mm by 7mm in x and y axis in the glass interposer PDN. By adding the patches, electromagnetic band-gap is generated around 2GHz with stopping bandwidth of 0.835GHz.

We then changed the dimensions of the power patch to find out the effectiveness of altering dimensions on electromagnetic band-gap. Fig. 7 shows effectiveness of altering the size of the power patch on the electromagnetic band-gap. Changing the dimension did not have great impact on the band-gap's stop band range. Since the dimension did not greatly affect the band-gap, we changed

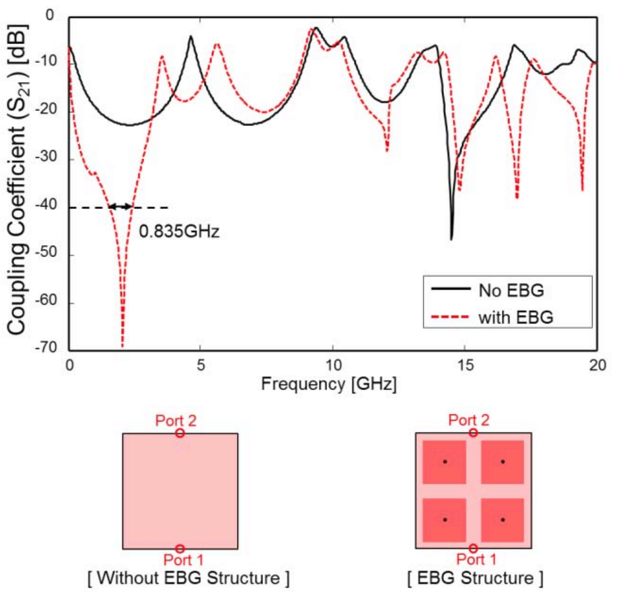


Fig. 6. Noise coupling coefficient with and without EBG (in this case, four additional power patch with 7mm by 7mm in are added in the PDN) is compared. Band-gap is formed around 2GHz and the stop band is 0.835GHz.

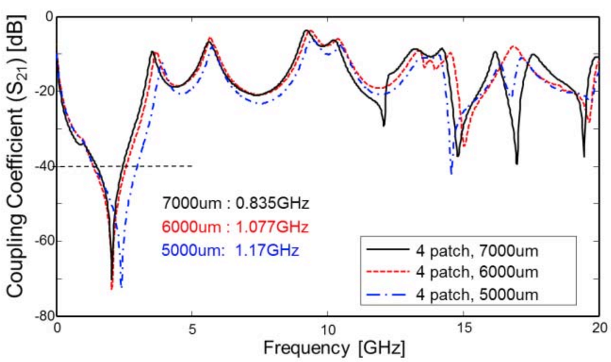


Fig. 7. Effectiveness of altering the size of the power patch on the electromagnetic band-gap was simulated. Changing the dimension did not have great impact on the band-gap's stop-band.

the number of power patches. However as can be seen from fig. 7, changing the dimensions of the power patch did not have great impact on altering the band-gap region. Therefore, we change the number of patches. Since the size of power and ground plane is fixed to 16mm by 16mm, we had to reduce the size of single patch when we increased the number of patches. In fig 8, impact of altering the number of patches on the electromagnetic band-gap is shown. Underneath the graph, dimensions are given with figures. By increasing the number of patches to 16 from 4, start frequency of the noise rejection region shifted down to lower frequency and stop frequency of the rejection region moved up to higher frequency range resulting in widening

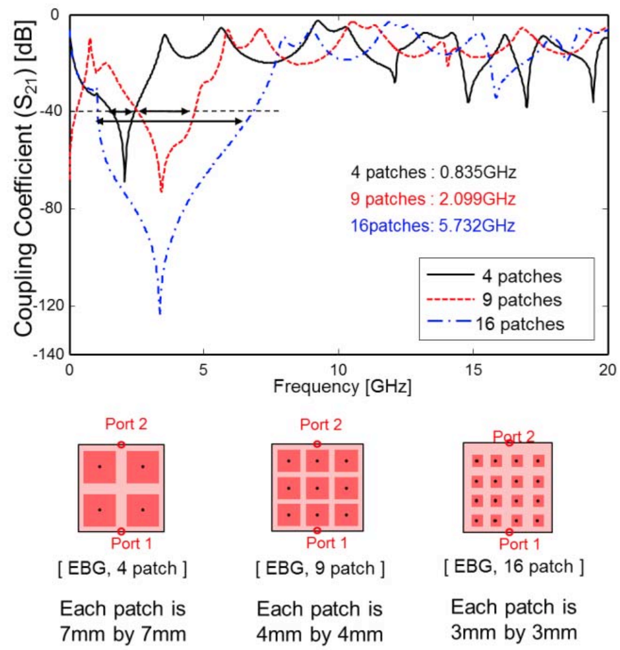


Fig. 8. Impact of altering the number of power patches on electromagnetic bandgap is shown.

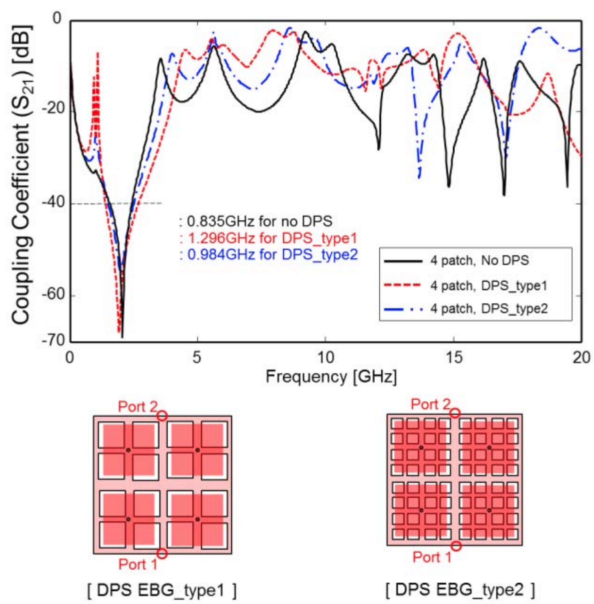


Fig. 9. Impact of defects in the power plane on the electromagnetic band-gap is shown.

the electromagnetic band-gap. With 16 power patches, band-gap are increased 6 times more than that of case with four patches. Since 2.4GHz and 5GHz frequency-ranges are important since operating frequency of Bluetooth and Wi-Fi remain in these ranges. Communication circuits are very vulnerable to noise coupling therefore 2.5D IC based on the glass interposer with mixed signal ICs may need to adopt EBG structures for the noise propagation suppression.

We also added some repeating defects in the power plane. If there exist voids in the power plane, capacitance of the PDN's unit cell will decrease and at the same time, resistance and the inductance will increase. Therefore, filtering characteristics of the unit cells will change, resulting in affecting the stop-band of the electromagnetic band-gap. Fig. 9 shows impact of defects in the power plane on the electromagnetic band-gap. We fixed the number of power patches to four with 7mm by 7mm in dimension. Under single patch, we applied uniform size of defects in the power plane. By increasing the number of defects under one power patch, band-gap increased with fixed center frequency up to certain point. Therefore when designing the electromagnetic band-gap in the glass interposer PDN, controlling the number of power patches had significant effect on the stop-band. Also by adding the repeating and uniform defects in the power plane, band-gap was increased.

## IV. Measurement of the Electromagnetic Bandgap in the Glass Interposer PDN

As mentioned in the earlier section, we designed glass interposer coupon with various types of EBG test vehicles. Among many test vehicles, we measure three test vehicles with good fabrication yield; plane type PDN, PDN with mushroom type EBG (25 power patches) and PDN with mushroom type EBG (25 power patches) and defects.

Fig 10 compares measured electromagnetic band-gap of glass interposer PDN with and without EBG structures. By adding a EBG structure, noise suppression band is formed with stop-bandwidth of 4.17GHz. In fig. 11, mushroom EBG structures with and without defects in the power plane are measured respectively. By adding defects in the power plane, band-gap became wider. This kind of tendency is also reported in the previous section via 3D EM simulation. Proposed structures work well as an electromagnetic band-gap in the glass interposer PDN.

## V. Conclusion and Further Works

In this paper, we designed electromagnetic band-gap structures in the glass interposer PDN. We conducted case studies of designed EBG structures with 3D EM simulation. We designed mushroom type EBG in the glass interposer PDN. We first changed the dimensions of the power patches that form mushroom type EBG with fixed number. However this did not have greatly changed the band-gap. It is more effective to change the number of patches. Also by adding the repeating defects in the power plane, noise isolation band increased. This tendency was also proved by measuring the fabricated test vehicle. In the later studies, models that can accurately predict these stop-bands in the glass interposer PDN are needed.

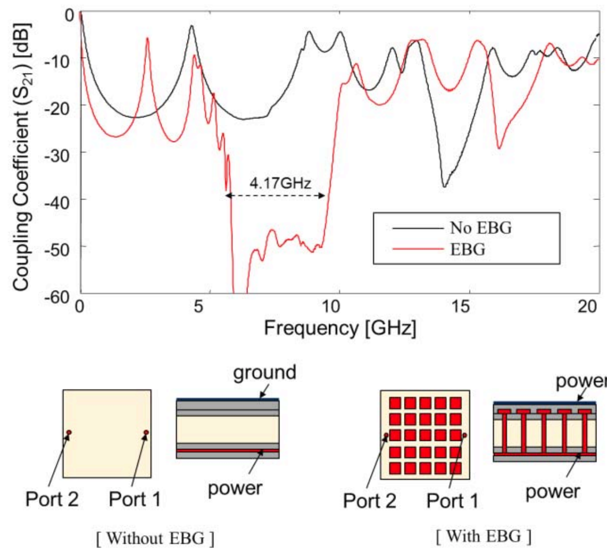


Fig. 10. Measurement of electromagnetic bandgap in the glass interposer PDN with and without mushroom type EBG structures (25 patches)

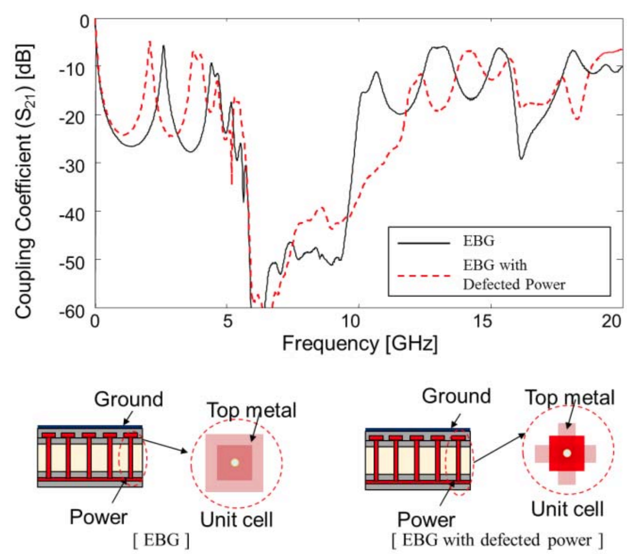


Fig. 11. Measurement of electromagnetic bandgap in the glass interposer PDN with and without defected power in mushroom type EBG structures (25 patches)

## Acknowledgment

This work was supported by International Collaborative R&D Program (funded by the Ministry of Trade, Industry and Energy (MKE, Korea) [N0000899, Glass interposer based RF FEM for Next Generation Mobile Smart Phone] also we would like to acknowledge the financial support from the R&D Convergence Program of MSIP (Ministry of Science, ICT and Future Planning) and ISTK (Korea Research Council for Industrial Science and Technology) of Republic of Korea (Grant B551179-12-04-00). We also like to acknowledge the technical support from ANSYS for providing 3D-EM simulator HFSS.

## REFERENCES

[1] V. Sukumaran, T. Bandyopadhyay, V. Sundaram, R. Tummala, "Low-Cost Thin Glass Interposers as a Superior Alternative to Silicon and Organic Interposers for Packaging of 3-D ICs," *IEEE Transactions on Components, Packaging and Manufacturing VOL. 2, NO. 9, September 2012*

[2] Venky Sundaram, Quio Chen, Yuya Suzuki, Gokul Kumar, Fuhan Liu, and Rao Tummala, "Low-cost and low-loss 3D silicon interposer for high bandwidth logic-to-memory interconnections without TSV in the logic IC," *Electronic Components and Technology Conference (ECTC), 2012 IEEE 62nd, pp.292,297, May29 2012-June 1 2012*

[3] J.S.Pak, C. Ryu and J.Kim, "Electrical characterication of through silicon vis depending on structrual and material parameters based on 3-D full wave simulation", *in Proc. IEEE , Electron. Mater. Packag., Nov. 2007, pp.1-6*

[4] Y. Kim, K. Kim, J. Cho, V. Sundaram, R. Tummala and J. Kim, "Analysis of Power Distribution Network in Glass, Silicon Interposer and PCB," *in Proceedings of the 2014 IEEE International Symposium on Electromagnetic Compatibility, Raleigh, NC, August 5, 2014*

[5] K. Kim, J. Yook, J. Kim, H. Kim, J. Lee, K. Park, and J. Kim, "Interposer Power Distribution Network (PDN) Modeling Using a Segmentation Method for 3D ICs With TSVs," IEEE Transactions on Components, Packaging and Manufacturing Technology, Vol. 3, No. 11, pp. 1891-1906, November 1, 2013.

[6] J. Kim, W. Lee, Y. Shim, J. Shim, K. Kim, J. Pak and J. Kim, "Chip-Package Hyierachical Power Distribution Network Modeling and Analysis Based on Segmentation Method," IEEE Transactions on Advanced Packaging, Vol. 33, No. 3, pp. 647-659, August 1, 2010.